ISSN 2349-7815

International Journal of Recent Research in Electrical and Electronics Engineering (IJRREE)
Vol. 2, Issue 1, pp: (32-53), Month: January - March 2015, Available at: www.paperpublications.org

Inverter for Fuel Cell Based On PWM Cycloconverter

[1]Deepa Zamwar, [2]Jitendrasingh Bhadoriya

[1]Final Year Student, M. Tech., RGPV University Bhopal, India,
[2]Asst.prof. NRI College Bhopal, India

***Abstract*: A low-cost high-performance fuel cell inverter for nominal 48 V dc to 120 V ac conversion is described. The inverter topology eliminates the need for a dc intermediate voltage by using an ac-link output inverter. The design minimizes overall system cost – including energy storage and management. The design provides low-ripple current-controlled interfacing to the fuel-cell stack, an intermediate-voltage battery energy storage buffer, and an ac-link output inverter. The circuit is based on square-wave cycloconverter technology, combined with a simple approach modulation process. Number of stages and magnetic elements low while providing galvanic isolation. Either SCRs or IGBTs can be used as output devices, which provides an unusual cost/performance trade-off possibility. Gate drives and other control elements are also simplified. The design provides excellent performance with a minimum of filter components and a simple control.**

***Keywords*: PWM, Cycloconverter, Inverter, Simulation, Multivibrator, Fuelcell.**

1. INTRODUCTION

For the power conversion system where linkage with ac system line is required, the HF (high-frequency) link converter topology has been attracting special interests recently, because it enables the power converters to be compact and light-weight. Two types are considered in the high frequency converters. One is a dc/dc converter type and other is a cycloconverter (ac/ac) type.

This paper details the application of low cost fuel cell inverter using multiple carrier PWM for ac-ac converter. The power conversion is more direct (two stages).Also PWM cycloconverter, with or without natural commutation, and conventional PWM inverter is unified through a multiple carrier PWM framework. Issues about complexities are resolved. Multiple carrier PWM methods lead HF link inverters that are about as simple as conventional PWM inverter.

The visions of a fuel cells potential are diverse. They include fuel cells powering cars, operating as backup or even primary power for your home from a shed-sized fuel-cell system, and providing power for larger commercial buildings and computer installations. Such systems can produce significant power. Though practical model is build but with some minor modifications commercial fuel cell inverter can be built.

2. OVERVIEW OF SCHEME

Fuel Cells:

Fuel cells combine hydrogen (or other oxidiazable fuel), oxygen, and an ionic conductor electrolyte to produce electrochemical oxidation. The results are oxidized fuel – such as water – and electric current. Because the reactions are electrochemical rather than thermal, the energy conversion efficiency can be very high. The operation is similar in many ways to that of a battery. The primary exception is that a continuous fuel source is provided to keep the reactions going indefinitely.

ISSN 2349-7815

International Journal of Recent Research in Electrical and Electronics Engineering (IJRREEE)
Vol. 2, Issue 1, pp: (32-53), Month: January - March 2015, Available at: www.paperpublications.org

2.1.1 Chemistry and Characteristic of Fuel Cell :

Fig.1 provides a static current-voltage relationship for a prototype fuel cell. This particular curve is taken from a proton exchange membrane (PEM) fuel cell model. PEM fuel cells use hydrogen as the fuel source and have an open circuit voltage of 1.15 V per cell at 80^0 C and one atmosphere of pressure.

Under load, the voltage drops abruptly and is typically 0.6 V per cell or even less. It is important that the working voltage be high enough to remain to the left of the "knee" in the curve, which occurs at about 9A in Fig.1. A fuel cell stack with 64 cells in series, based on Fig.1, would have open-circuit voltage of 74 V and operating voltage of about 40 V. To support the operation of the fuel cell stack, there will be a parasitic load for pumps, fans and other equipment typically of the order of $1/6^{th}$ of rated load. In Fig.1, this balance of plant load implies an actual working voltage range of 0.5 to 0.8 V per cell. The power processing system must be able to handle this range and withstand the open-circuit voltage during startup conditions. In practice, a fuel cell stack with 64 cells would generate a working range of 32 to 52 V. There are significant dynamic issues that must be addressed in any system. The dominate issues relate to fuel flow and transient response.

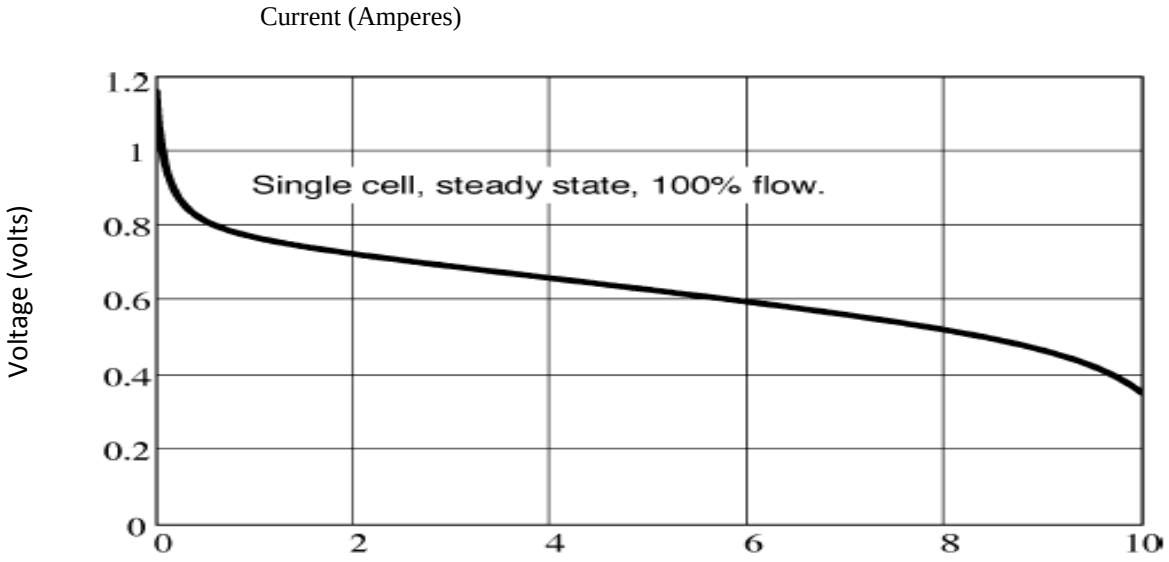

Fig. 1 Typical Fuel Cell Voltage-Current Characteristic

Fig.1 shows the behavior with 100% rated fuel flow in a flow-through type of system, but it does not reflect efficiency considerations. For example, if the cell in Fig.1 operates at 2 A (about 25% of rated load) with 100% fuel flow, only a small fraction of the fuel will actually participate in the electrochemical reaction. In a vented flow-through stack, the remainder will be sent, unused, out the exhaust. Since direct recovery of hydrogen from the exhaust is difficult, wasted fuel represents very low efficiency.

Other operating methods might use constant fuel pressure, in which case diffusion rates and oxygen supply limit the performance. In a practical system, the fuel flow (or target is pressure) must be adjusted to match the reactant delivery rate to the usage rate. A typical fuel utilization of at least 85% to avoid excessive waste.

2.2 Fuel Cell with Battery:

Fig.2 shows three of the family of curves that result when fuel flow is taken into account. In a flow-through PEM system, for a given electrical load, the fuel flow should be adjusted to give the proper match. This causes two problems. First, flow rates cannot be adjusted rapidly, and the internal chemistry must reach equilibrium before the cell can support increased load. Second, if the electrical load increases too rapidly, it could drive the curve over Fig.1. Typical fuel cell voltage-current characteristic the knee, exceeding maximum power transfer and overheating the fuel cell stack with extra losses. The dynamics of fuel flow and diffusion of reactants are such that time constants associated with Fig.2 range from several seconds for PEM technology to several minutes for some other fuel cell technologies—not useful for following fast-changing electrical loads.

ISSN 2349-7815

International Journal of Recent Research in Electrical and Electronics Engineering (IJRREE)
Vol. 2, Issue 1, pp: (32-53), Month: January - March 2015, Available at: www.paperpublications.org

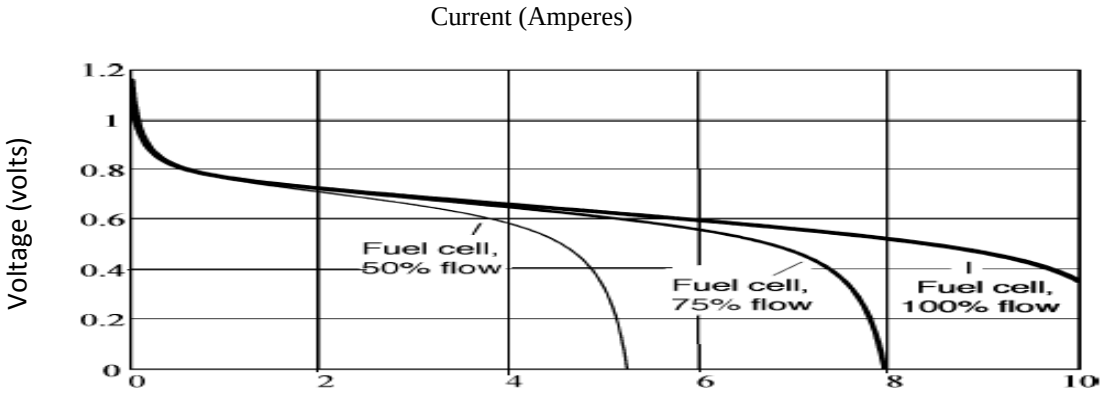

Fig.2 Voltage-Current Characteristics at Several Different Fuel Flow Levels

In any application with an uncontrolled electrical load, an energy buffer such as a separate battery will be needed to permit instantaneous response to electrical load shifts while the fuel cell stack catches up.

However, based on Fig.2, it will not be feasible to simply add batteries in parallel with the stack. A battery – curve is similar to a fuel cell and the operating point cannot be managed with a direct parallel connection, especially as fuel flow rates change. In practice, this requires that a dual-port converter will be required to allow both a fuel cell and a battery to be used independently. A battery will also require bidirectional energy flow to maintain charge over long intervals. Convention dictates that fuel cells are intolerant to ripple current. Upon first examination, the physical structure of a fuel cell is similar to that of an electrolytic capacitor, and fuel cells in general have significant internal capacitance. However, since the electrochemistry is not perfectly efficient, internal losses limit the ability to withstand the extra losses caused by ripple current. In addition, ripple current at relatively low frequencies will perturb the operating point and could drive instantaneous operation beyond the knee of the characteristic curve. Thus a typical fuel cell is relatively intolerant to current ripple at low frequencies of 120 Hz or less but is more forgiving of higher frequency ripple at several kilohertz or more.

One challenge with a fuel cell is that the reaction rate is controlled in part by delivery of fuel. The fuel must be delivered at least as fast as it is consumed, but fuel is wasted if the delivery rate is faster. In a practical system, this means that a fuel cell looks like a battery with very slow dynamics: the time rates of change associated with sensors, pumps, fans, and the system exhaust means that the fuel cell controller requires approximately one minute to respond to a command for change, and about 90 s for initial start.

In an inverter system, the ac side load will have dynamics much faster than this, so an energy storage buffer will be necessary. At a given fuel flow rate, a fuel cell has an optimum output current – that current will provide the highest output power while minimizing losses and internal wear and tear. This behavior is somewhat similar to that of a solar cell, although it is usual to operate a fuel cell at a current slightly below its maximum power output point to keep reliability high. In the end, current optimization means that a precise average current control is needed for the fuel cell itself.

Fuel cells produces relatively low voltage – a fraction of a volt per cell – since the voltage is related to the electrochemical potential of an H2 - O2 reaction. It is possible in principle to draw energy directly from an individual cell. But the realities of device voltage drops and extreme currents mean that a single cell does not provide efficient energy conversion. To alleviate this limitation and to achieve practical voltage levels, many cells must be connected in series. This gives rise to the complete "fuel cell stack." In general, any voltage can be achieved by stacking cells in series, but in the event of a single-cell failure or degradation, the entire stack will be affected. Thus there is an "optimum voltage" with some cells in series (but not too many). Although this optimum voltage has not been studied rigorously as yet, conventional battery and solar cell practice suggests a level from 20 V to 60 V as a realistic value. Choose a nominal 48 V cell stack as the input to reflect this expectation.

System electrical safety is an issue. However, since it is possible to provide a safe enclosure for a unit, electrical safety is somewhat secondary. Most standards practice accepts dc voltages under 60 V as a safe level not subject to special protection requirements. On this basis, a 48 V fuel cell stack has important advantages – the open-circuit output when

pumps and other necessary hardware are in place is unlikely to exceed 60 V. It is relatively easy to assemble a 48 V fuel cell stack into a system that is safe enough for residential use.

A 48 V output is not enough to achieve a useful ac output voltage therefore a step-up function will be required. The only way to achieve highly efficient energy conversion from 48 V dc to conventional 120/240 V ac is to use the techniques of power electronics switching devices and energy storage elements to perform dc to ac conversion. However, the objective of this project is not just to make power electronic circuits, but also to make them at low cost and to give them high reliability.

2.3 Interfacing of Fuel Cell:

The source impedance characteristics shown in Fig.1 and 2 and the desire to operate the fuel cell at a specific "fuel utilization" level suggest current control as the appropriate interface with the fuel cell. The input current can be set at any moment to the ideal value for the available fuel flow and the maximum current ripple is determined by design.

The current commanded from the fuel cell as well as the fuel flow rates can be adjusted to track the average output power requirements of the inverter as the average electrical load changes. Batteries can be provided as a supplement to respond to fast load variation.

The arrangement could be as simple as a boost converter cascaded with an inverter bridge. But what about the batteries? In principle, they can be connected at the high-voltage dc bus. While a high-voltage battery is a simple approach, it raises its own problems. Batteries in the range needed (more than 300 V) are difficult to manage. It is especially difficult to maintain a tight charge balance [3], and it is unlikely that this could become a practical solution.

2.3.1 General Requirements:

The conversion topology must achieve several specific engineering objectives:

• Current control for the fuel cell must be supported. Precise control of current with minimum low frequency ripple is needed.

• The fuel-cell current control must be decoupled from the rest of the system. That is, the current must be fully controlled independent of the ac load.

• Energy storage must be provided to support decoupling between the fuel cell and the load, so rapid load changes do not affect the fuel cell.

• A high-quality two-port sinusoidal output is needed.

2.3.2 Inverter with Step-up Transformer:

From a conceptual viewpoint, there are two general approaches that can be taken to this inverter problem**:**

Convert the energy from the fuel cell into ac form, and then step this up to produce the desired output. An example is given in Fig3.

The trouble with this approach is that the transformer will have to be rated for the 50 Hz hence will require a bulky mains-frequency transformer and will yield a heavy system with little opportunity for cost reduction. However, it offers the advantage of galvanic isolation.

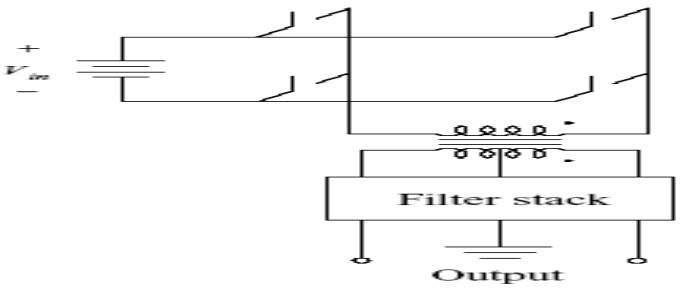

Fig.3 Direct Low-Voltage Inverter Followed by Transformer Step-up

ISSN 2349-7815

International Journal of Recent Research in Electrical and Electronics Engineering (IJRREEE)
Vol. 2, Issue 1, pp: (32-53), Month: January - March 2015, Available at: www.paperpublications.org

2.3.3 DC–DC Converter Cascaded With Bridge Inverter:

Use a dc-dc conversion approach to step up the voltage (perhaps at high frequency), then use a conventional inverter to produce the ac output. In concept, this approach can be treated as a conversion from dc to high-frequency ac, a rectification to high-voltage dc and inversion to 50 Hz as in Fig.4 which involves a cascading of power conversion stages, each of which adds loss. Eliminating the line frequency transformer reduces the size and weight but also eliminates galvanic isolation.

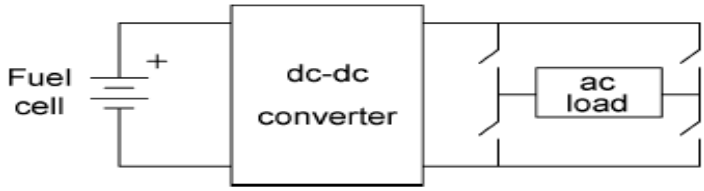

Fig4 dc–dc Converter Cascaded with Bridge Inverter

In general terms, the conversion process can be treated as a cascade of a step-up from the fuel cell stack and a conventional inverter, as in Fig.4. This is a boost converter cascaded with an inverter bridge. This arrangement does not provide operational decoupling between the fuel cell and the inverter. In addition, the boost gain needed for the circuit of Fig.2.4 is extreme. A gain of more than 7 from input to output must be achieved at high power with high efficiency. Such extreme gains place severe requirements on the filter components, and seem unlikely to be practical.

2.3.4 Two Input Current Sourced Forward Converter:

The fuel cell and the batteries can be treated as two, more or less independent inputs to the boost converter – in the form of a current-sourced forward converter. Fig.5 shows a current-sourced converter that can meet with the basic requirements.

The general concept is that of a current-sourced forward converter, followed by a simple voltage-sourced inverter bridge.

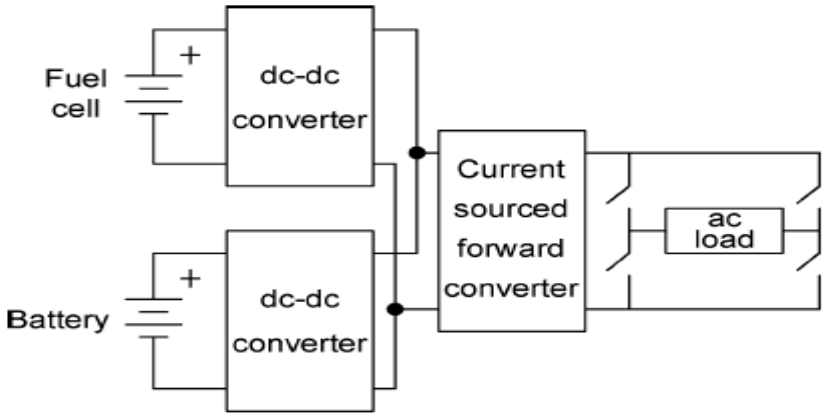

Fig5 Two-Input Current-Sourced Forward Converter as the Basis for the Fuel Cell System

The concept in Fig.5 is viable, but has a number of challenges that prevent it from becoming a low-cost solution. First, four significant magnetic elements are needed: two input side inductors, the forward converter transformer, and an output-side filter inductor (inside the “ac load” block). Second, the battery conversion portion must be bidirectional to support both charge and discharge. The inverter bridge does not support dual output ports, although it permits either a voltage-sourced inverter approach or a PWM inverter control.

An advantage of the approach is the redundancy of the fuel cell and batteries: operation can take place with just one source connected. Another advantage is high efficiency: the batteries do not have to act as an intermediate energy source if power can flow directly to the load. The most significant issue in configuration of Fig.5 is that of control decoupling. In

ISSN 2349-7815

International Journal of Recent Research in Electrical and Electronics Engineering (IJRREE)
Vol. 2, Issue 1, pp: (32-53), Month: January - March 2015, Available at: www.paperpublications.org

principle, the battery current can be chosen to exactly cancel dynamics of the inverter load to ensure constant current drawn from the fuel cell. In practice it is hard to do this precisely.

Since the fuel cell supplies the forward converter directly, any change in the ac-side current will alter the fuel-cell current unless control action is instant.

2.3.5 Forward Converter Driving Batteries and Inverter:

Fig.6 shows the other way of connecting the battery. This is the same as Fig.5, except that the battery has been moved to the forward-converter output bus.

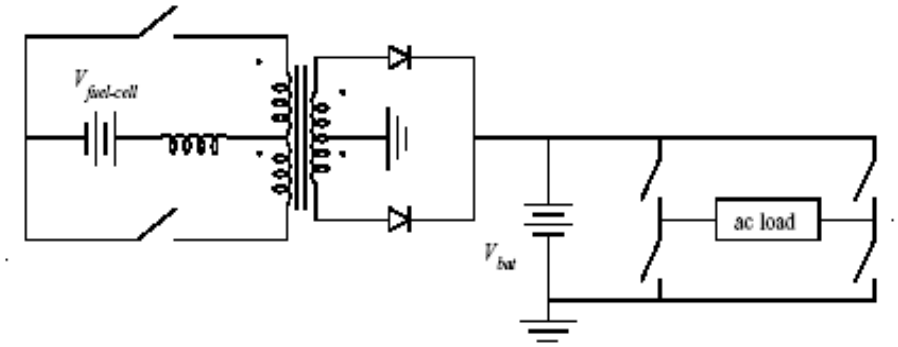

Fig.6 Forward Converter Driving Batteries and Inverter

Fig.6 is extremely simple and has considerable appeal, but from a system-level cost perspective it is flawed. The battery bus will need to have a nominal value of about 340 V, which requires series connection of 28 lead-acid batteries. This long series connection is not out of the question, but the charging of a long series string leads to imbalance problems .

Above approach is more expensive but commercialized. In either case, it would be preferable to minimize the imbalance problem and avoid the cost of an extensive battery balancing network and wire harness.

2.3.6 Three Stage Converter Boost/Forward/ Inverter:

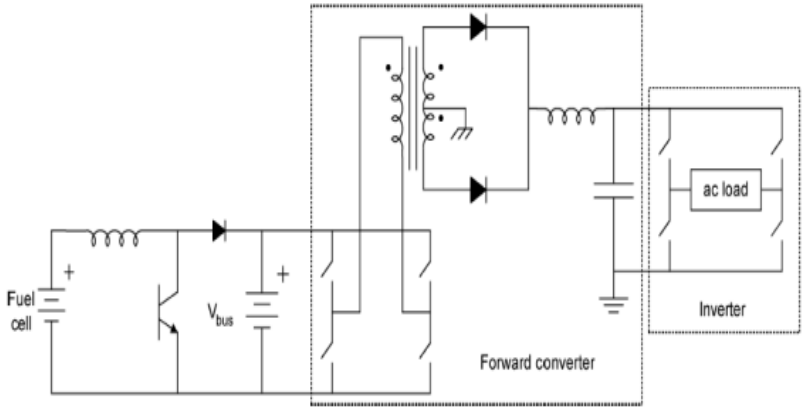

Fig.7 Three-Stage Converter: Boost/Forward/Inverter

Fig.7 shows a boost converter, followed by a voltage-sourced forward converter and inverter. A key advantage of this topology is decoupling of control: the boost converter can act to maintain the desired current from the fuel cell, independent of the forward converter action or of the inverter. There are two major troubles with this topology: First, the extra diode in the boost converter reduces efficiency compared to the two-port converter approach (Fig. 5). Second, addition of one conversion stage. Although the number of components has not changed much in terms of complexity circuit of Fig.7 and Fig.5 are at par.

ISSN 2349-7815

International Journal of Recent Research in Electrical and Electronics Engineering (IJRREE)
Vol. 2, Issue 1, pp: (32-53), Month: January - March 2015, Available at: www.paperpublications.org

In Fig.7, there are three sets of controls: the initial boost converter control, the forward converter control, and the inverter control. Furthermore, the power conversion blocks proceed from the current sourced fuel-cell input, to the voltage-sourced battery bus.

This stack up of sources can be reduced, since at least one source is redundant.

2.3.7 Boost Converter Followed by ac Link Inverter and ac-ac Converter:

Reduction of redundancy will eliminate a portion of the control as well as the extra stage. The concept is embodied in a high-frequency link arrangement, shown in Fig.8

The proposed design actually uses a third approach, based on ac link cycloconversion method. This eliminates the rectification stage and performs inversion directly, simplifying the system.

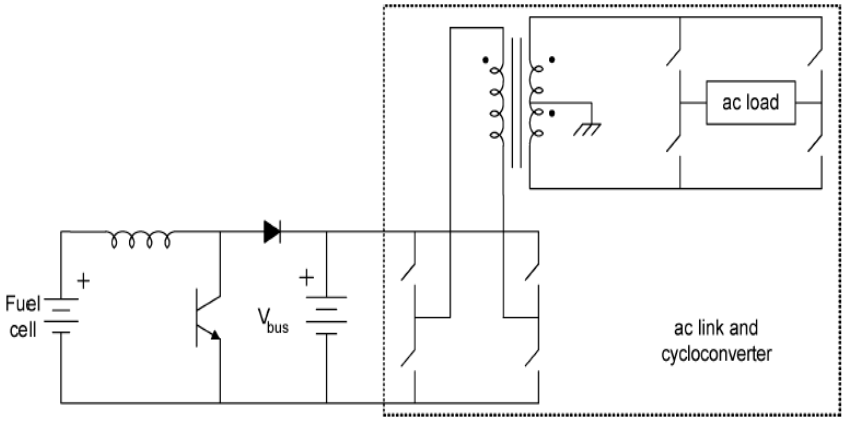

Fig.8 Boost Converter, Followed by ac Link Inverter and ac-ac Converter for Output

This configuration is combination of boost converter, followed by ac link inverter and ac-ac converter for output. Forward converter is replaced with a simple square-wave inverter which delivers a square-wave voltage to the output bus. The inverter is replaced with an ac-ac converter to deliver the 50 Hz output. In this sense, the ac link approach leads to a cycloconverter-type system, in which a square wave ac input is chopped to deliver the desired output.

Cycloconversion techniques are rarely used because of the control complexity, problems with devices, and poor output harmonic characteristics. These limitations are not really fundamental: it is possible to produce the desired output waveform directly from the ac link stage without the problems of a cycloconverter by using a new way to perform pulse-width modulation (PWM) that actually produces a cycloconverter with a standard PWM output.

Block diagram for the scheme. Input is 24V battery/fuel cell with capacitor for filter. Inverter is of push pull configuration with 1 KHz frequency. Cycloconverter is having 50Hz frequency. Isolation is obtained from high frequency transformer.

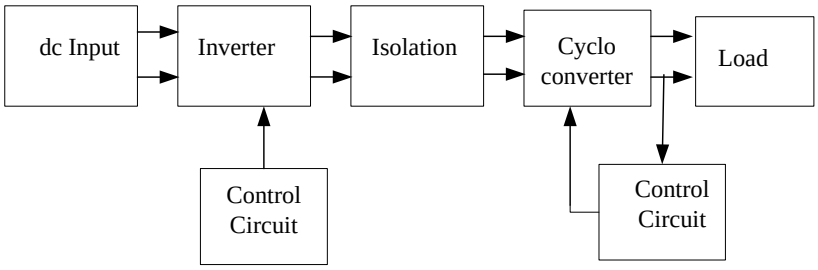

Block Diagram

i. Control Block for Inverter:

Gate pulses are applied to switches of push pull inverter. Phase delay is introduced between pulses as Shown in Fig 9. Gate pulses are in synchronization with 2 KHz ramp.

ISSN 2349-7815

International Journal of Recent Research in Electrical and Electronics Engineering (IJRREEE)
Vol. 2, Issue 1, pp: (32-53), Month: January - March 2015, Available at: www.paperpublications.org

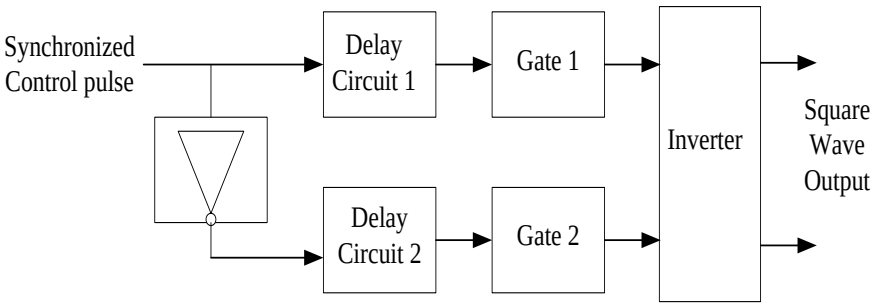

Fig.9 Control Block for Inverter

ii. Control Block for Cycloconverter:

For control block Multiple Carrier PWM scheme is used. In this high frequency carrier is used along with modulating signal. Carrier could be triangle or ramp. Modulating signal is low frequency component. For multi carrier operation instead of two carriers two modulating signals are taken which solve the purpose and is valid for single phase cycloconverter. Carrier is 2 KHz ramp and modulating signal is 50Hz sine wave. Control is applied to cycloconverter side while inverter gate pulses are synchronized with ramp at 1KHz.

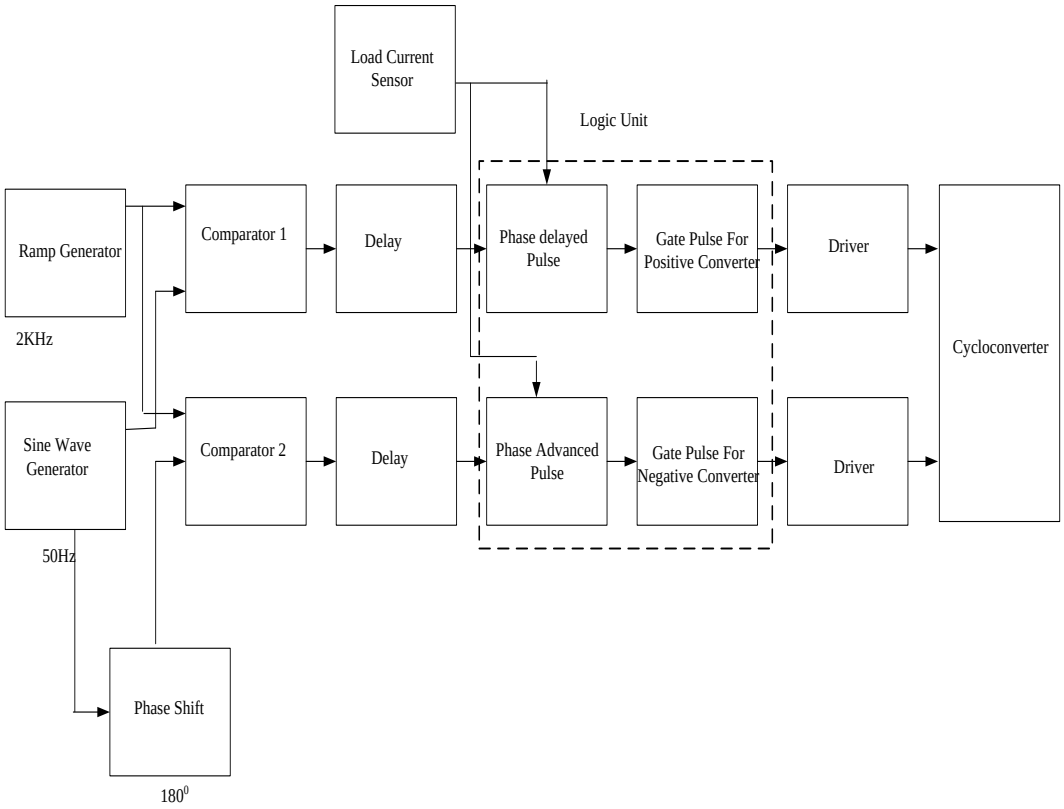

Fig.10 Control Block for Cyclconverter

As shown in Fig.10 control module contains ramp generator of frequency 2KHz which also gives square wave of 1KHz to be applied as control for forward converter i.e. inverter.

Sine wave obtained at 50Hz is modulating signal. For multiple carrier operation this sinusoidal waveform is phase shifted by 180^0.

By comparing carrier and modulating signal PWM output is obtained. This PWM output is advanced or delayed for achieving phase advanced and phase delayed trigger pulses respectively. Such pulse train is obtained using multivibrator

The delayed waveform is blanked when the current is negative, while the advanced waveform is blanked when the current is positive.

The two multivibrators are triggered from the rising edge of the respective comparator to produce a 15μs gate pulse train. The upper multivibrator creates a phase-delayed gate pulse train to be used when load current is positive, while the lower multivibrator creates a phase-advanced gate pulse train to be used when the load current is negative. Simple logic is used with a current comparator to separate the positive and negative current conditions.

These trigger pulses are combined with another input obtained from current polarity detector. This current polarity detector detects current direction across load.

Thus trigger pulses obtained are applied to positive and negative converter of cycloconverter through driver.

iii. Power Block:

Power block is described under two sections, as this consists of primary side and secondary side with isolation as shown in Fig. The primary side, inverter operation is obtained through push-pull configuration while output is single phase bridge consisting of 8 SCRs connected in antiparallel. RC snubber is designed for switches.

iv. Inverter:

As shown in Fig, inverter consists of push pull inverter which converters 24V dc to 96Vp-p, 1 KHz square wave. This push pull inverter uses two MOSFETs as switches. Driver for MOSFET is obtained by transistorized circuit. Driver signals are synchronized with 2 KHz ramp. Inverter switches at 1KHz. Filtering of dc voltage from battery is done through capacitor.

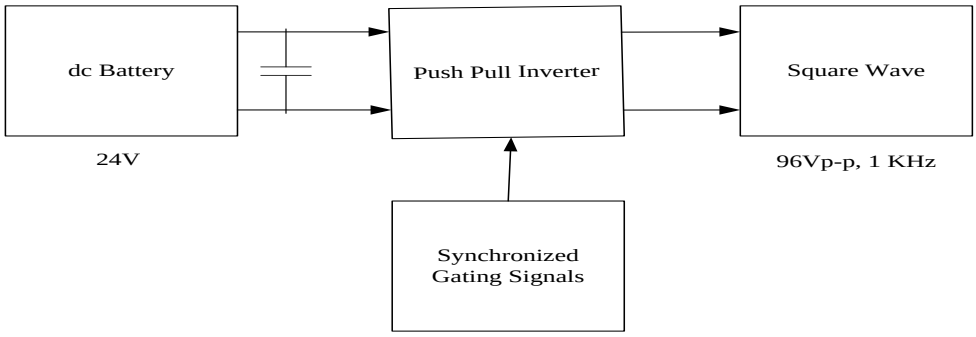

Fig.11 Inverter

v. Cycloconverter:

Fig.12 shows schematic for ac-ac converter along with current polarity detection. Commutation of cycloconverter during the zero crossing of load current is an important control issue, well understood from conventional ac cycloconverter results. Ideally, the current polarity detection scheme in Fig.5 would use the "fundamental current zero". While this scheme results in ideal commutation with no cross-over distortion, it is known to be difficult to implement in practice. Instead, Fig.5 uses a modification to the "first current zero"

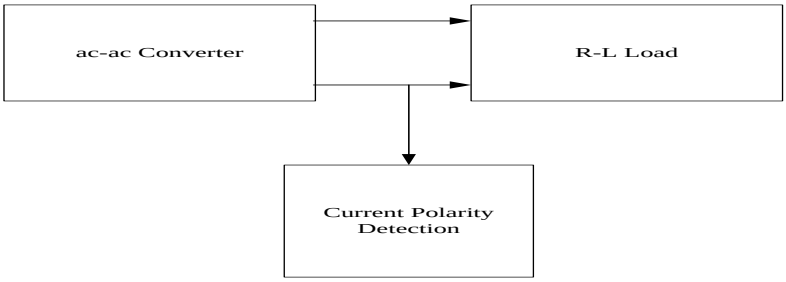

Fig.12 Cycloconverter

As shown in block diagram secondary of power module consists of single phase ac-ac converter with 8 SCRs along with 4 RC snubbers. Load connected is RL and switching is controlled from trigger pulses obtained from control module whose feedback is from current polarity detector, which senses the load fed from cycloconverter. Isolation between source and load is obtained using HF transformer. This transformer uses ferrite core to achieve high frequency square wave transfer.

3. DESIGN OF INVERTER CONTROL BLOCK

Synchronized square pulse is obtained which is phase shifted and delayed before applying to switches.

i. Design of Synchronized Square Pulse:

Synchronized square pulse is achieved from ramp generator as shown in fig. D flip flop IC4013 is used with reset on ON facility. Clock is given through non-inverting buffer consisting of CE amplifier with BC 546. Diode IN4148 is used as edge detector and for bypassing negative cycle.

IC4013 is used to generate square wave of 1 KHz synchronized with 2 KHz ramp. Clock frequency is also 2 KHz. The CD4013B dual D-type flip-flop is used.

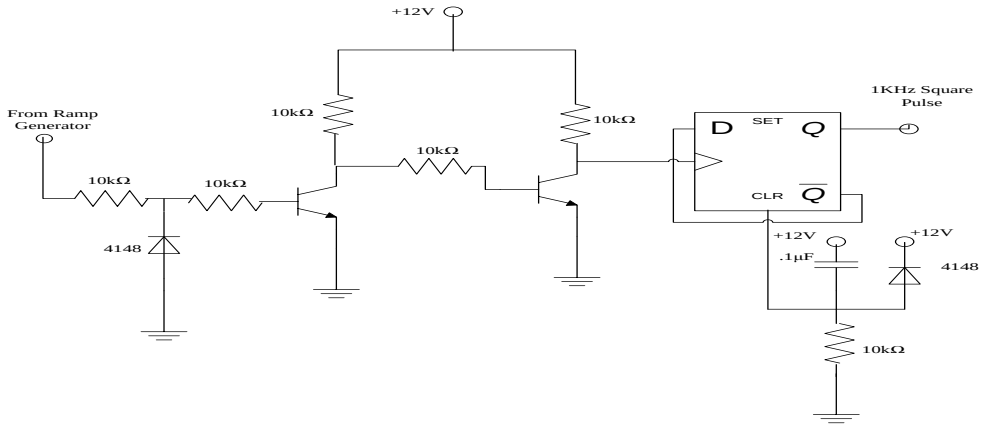

Fig.13 Synchronized Square Pulse

ii. Design of Gate Pulse:

The 50% duty cycle for gate pulses still support pulse transformer coupling, retaining the simplicity of the gate drive isolation. The PWM cycloconverter process scales directly to higher switching speeds possible with these devices. NAND gate IC 4093 is used for inversion in gate pulse. Delay is obtained using standard RC circuit.

R = 10 K Ω

C = 0.01 μF

R*C = 0.1ms

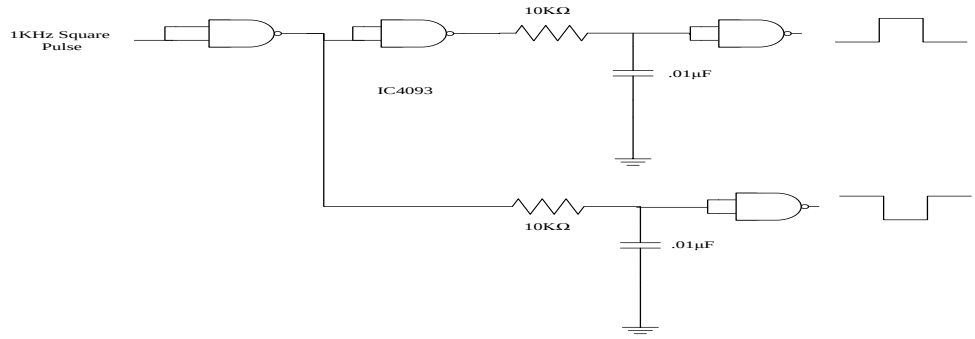

Fig.14 Gate Pulses for Inverter

ISSN 2349-7815

International Journal of Recent Research in Electrical and Electronics Engineering (IJRREEE)
Vol. 2, Issue 1, pp: (32-53), Month: January - March 2015, Available at: www.paperpublications.org

iii. Design of Ramp Generator :

Ramp Generator is achieved from triangular wave generator by inserting a variable dc voltage into the non-inverting terminal of the integrator A2 as shown in Fig.6. A duty cycle less than 50% causes output of A2 to be a ramp. When R4 wiper is moved toward –VEE, the rise time of ramp becomes longer than fall time. Also frequency of ramp is adjusted with R4. Amplitude of output is independent of R4.

Design is done for 7Vp-p, 2 KHz positive going ramp using op-amp [13]

fo = 2 KHz

R2/ R3 = Vp-p / 2*Vsat

Let Vp-p = 7V

R2 = 10 KHz

Vsat = 12V

R3 = 34.28 KΩ

Choose R3 = 22K+10Kpot

fo = R3/4 R1*C1*R2

R1*C1 = 0.4ms

Let C1 = 0.47µF

R1 = 851 Ω

Let R1 = 1KΩ

Where fo ---------Output frequency in Hz.

Vp-p--------- peak to peak output voltage

As shown in fig , buffering and amplification is obtained from 3A op-amp. 47 KΩ for high input impedance and combination of 6 KΩ and 1 KΩ resistance for dc level shift hence obtaining swing of ramp across zero. Final value adjusted to 3 Vp-p and 2.5 KHz frequency. Quad op-amp IC348 is used in circuit. LM348 is chosen for ramp generation

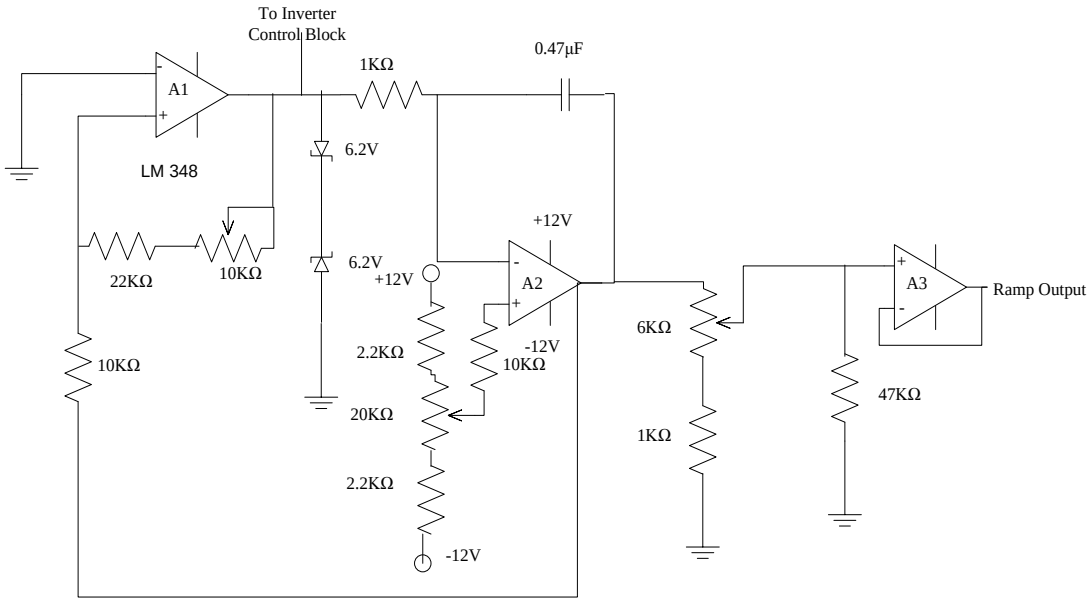

Fig.15 Ramp Generator

ISSN 2349-7815

International Journal of Recent Research in Electrical and Electronics Engineering (IJRREEE)
Vol. 2, Issue 1, pp: (32-53), Month: January - March 2015, Available at: www.paperpublications.org

a. Design of Sine Wave Generator :

Sine wave is obtained using bridge oscillator [13] as shown in Fig. Designing is done at 12Vp-p, 50 Hz frequency.

fo = 0.159/Rc

R*C =3.18ms

Let C = 0.47 µF

R = 6.7 KΩ

Gain Rf '[/ R1 = 2

Let R1=5.'1 KΩ

R1=5.1 KΩ

Rf = 10 KΩ

Rf = 10 KΩ pot

2 Vp-p is achieved using potential divider as shown in Fig. 9. Buffer is also connected. This sine wave is further inverted using op-amp as inverting amplifier. Gain for this op-amp is set as 1 with combination of 10 K and 9.1 K and 2K pot.

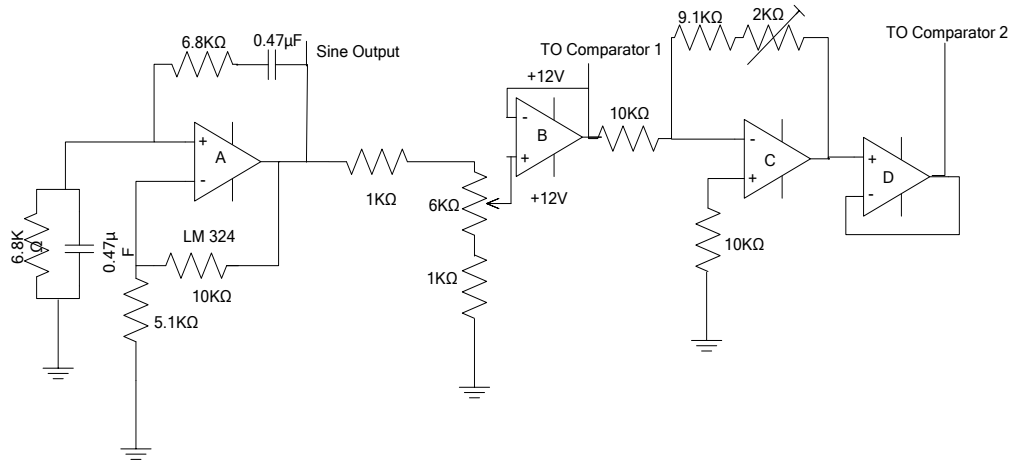

Fig.16

b. Design of Comparator:

For obtaining PWM comparison is done between ramp and sine using high speed voltage comparator dual comparator LM319. Modulation index is set to 0.66.

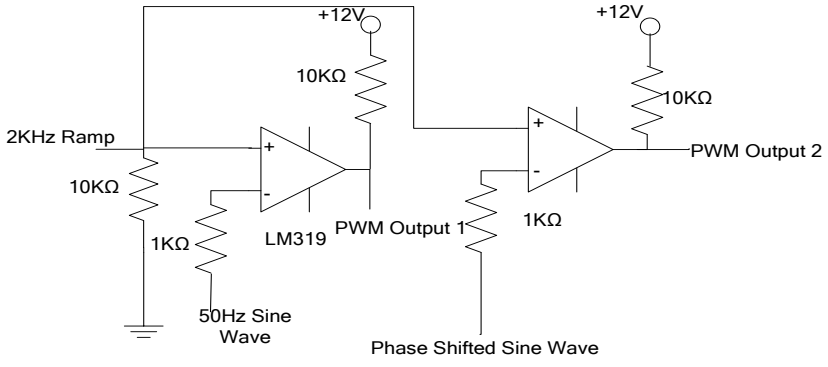

Fig.17 PWM Generator

ISSN 2349-7815

International Journal of Recent Research in Electrical and Electronics Engineering (IJRREEE)
Vol. 2, Issue 1, pp: (32-53), Month: January - March 2015, Available at: www.paperpublications.org

c. Design of Multivibrator:

The MC14538B is a dual, retriggerable, resettable monostable multivibrator. It may be triggered from either edge of an input pulse, and produces an accurate output pulse over a wide range of widths, the duration and accuracy.

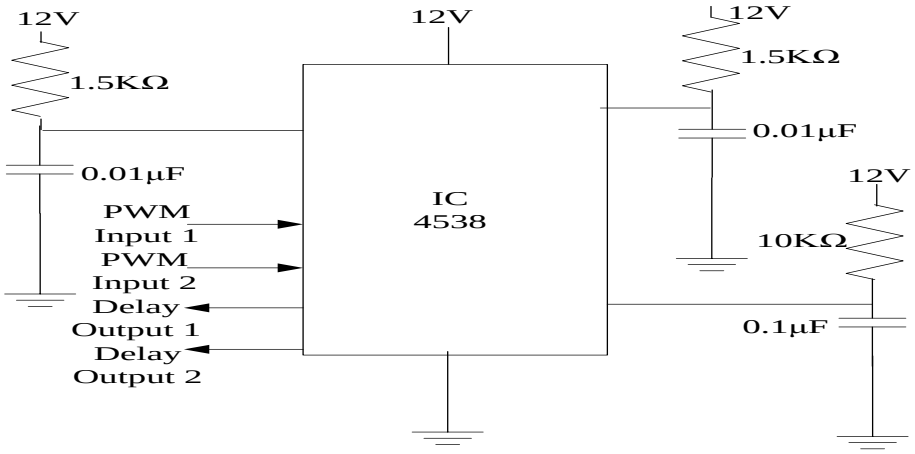

Fig.18 Delay Output

Of which are determined by the external timing components, CX and RX.

For 15µs delay value of CX and RX are chosen as 0.01µF and 1.5KΩ respectively.

d. Design of Logical Unit:

- Design for Delayed and Advanced circuit:

NOR (IC4001) logic is used for obtaining phase advanced and phase delayed trigger pulses.

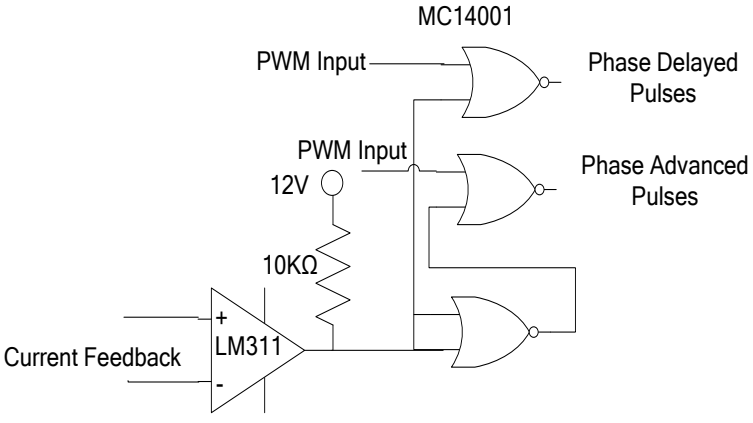

Fig.19.Circuit of Logical Unit

Design for Feedback Network - Single comparator is required for comparing feedback current obtained from load and PWM output obtained. Input is connected in differential mode as shown in Fig.19.

Both the inputs and the outputs of the LM311 can be isolated from system ground, and the output can drive loads referred to ground, the positive supply or the negative supply.

ISSN 2349-7815

International Journal of Recent Research in Electrical and Electronics Engineering (IJRREEE)
Vol. 2, Issue 1, pp: (32-53), Month: January - March 2015, Available at: www.paperpublications.org

e. Design of Driver:

The driver circuit of cycloconverter consists of Pulse Transformer and transistors along with diode and resistances. As cycloconverter is having SCRs as switches only edges are required for trigger. To obtain voltage level transistor is used as an amplifier. Standard configuration is applied for achieving trigger pulses as shown in Fig. Transistor BD139 is used as driver and BC546 as buffer. Such unit is used for each SCR.

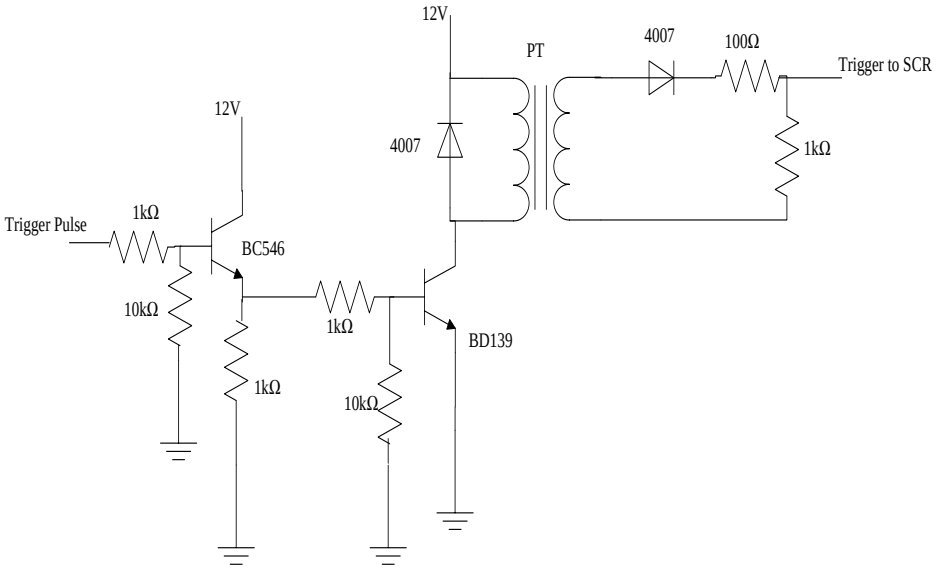

Fig.20 Driver of SCR

4. POWER CIRCUIT DESIGN

i. Design of Inverter:

Inverter is designed using push pull configurations and calculations are done as per requirement. Gate pulse is obtained from circuit shown in previous chapter. MOSFET is chosen for high frequency switching. Two 12V batteries are connected in series for obtaining 24V as fuel cell is not available. Batteries used are of standard company with 1A-Hr rating.

ii. Design of Push Pull Inverter:

24 Vdc is converted into square wave of 1 KHz frequency and amplitude of 48V at primary of output transformer using push-pull inverter. This is achieved by circuit shown in Fig.21.

Care is taken that switch has low saturation voltage and breakdown voltage is two to three times the supply voltage. Isolation is obtained through HF transformer which is described in the next section. Capacitor value 220μF/63V is connected across 24V battery for filtering.

Edc = 24V

Eout = 220V

Po = 200W

Io = 1A

Let η = 70%

Pin = 285W

Iin = Pin/Edc

=6A

ISSN 2349-7815

International Journal of Recent Research in Electrical and Electronics Engineering (IJRREE)
Vol. 2, Issue 1, pp: (32-53), Month: January - March 2015, Available at: www.paperpublications.org

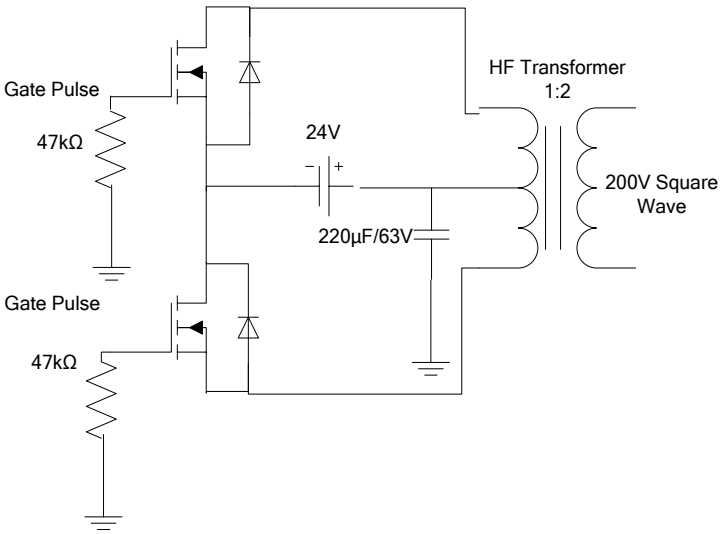

Fig.21 Push Pull Inverter

IRF540N Power MOSFET is used.

iii. Design of MOSFET Snubber:

fs = 1KHz

Edc = 24V

iL=6A

Let L = 25 µH

tf = 40x10-9 s

where

tf is fall time

fs switching frequency

C = iL*tf / Edc

= 6 * tf / 24

C = 0.01µF

L = Edc*tr / iL

tr = 6.25 µs

where tr is rise time

di/dt = iL/tr

= 0.96A/µs

Switch ON

di/dt = 0.24 A/µs

R = √(4*L/C)

R = 100 Ω

Hence values for snubber are chosen as 100 Ω,1W and 0.01µF/250V.

iv. Design of Transformer:

Ferrite core is used for transformer as operation frequency is 1KHz and input is Square Wave. Core is selected as per power requirement.

Edc = 24V

Eout = 220V

Po = 200W

Io = 1A

Let η = 70%

Pin = 285W

Iin = Pin/Edc

= 6A

As per calculations core required was EE-65x33x28 but due to its non-availability core used is EE-55x27x21 type 5s

Area = 20mmx17mm

N = Eout/Edc

= 5

$$Ns = \frac{Eout \times 105}{4 \times Bmax \times A \times f}$$

Bmax = 4800G

Br = 1800G

Hc = 11.9A/m

Let Bmax = 3150G

Calculating from above equation

Ns = 462

Np = 93

As push pull type hence each primary winding will have 93 turns each.

Maximum current rating is reduced due to core used.

v. *Design of ac-ac* Converter :

Secondary of high frequency transformer drives bridge of SCRs connected in anti-parallel and bridge is working as cycloconverter. SCRs are triggered from pulse transformer.

vi. Design of Cycloconverter:

As explained in a previous section current is approximately 1A hence SCR rating is chosen accordingly. As shown in Fig. eight SCRs are connected in anti-parallel to achieve ac-ac converter configuration. T1-T4 comprise of positive converter while T5-T8 comprise of negative converter.

SCR used is TYN612 having following features:

IT (RMS) -RMS on-state current (180° conduction angle) is 12 A

ISSN 2349-7815

International Journal of Recent Research in Electrical and Electronics Engineering (IJRREEE)
Vol. 2, Issue 1, pp: (32-53), Month: January - March 2015, Available at: www.paperpublications.org

VDRM/VRRM Repetitive peak off-state forward voltage is 600 to 1000 V

IGT Gate Current is 0. 2 to 15 mA

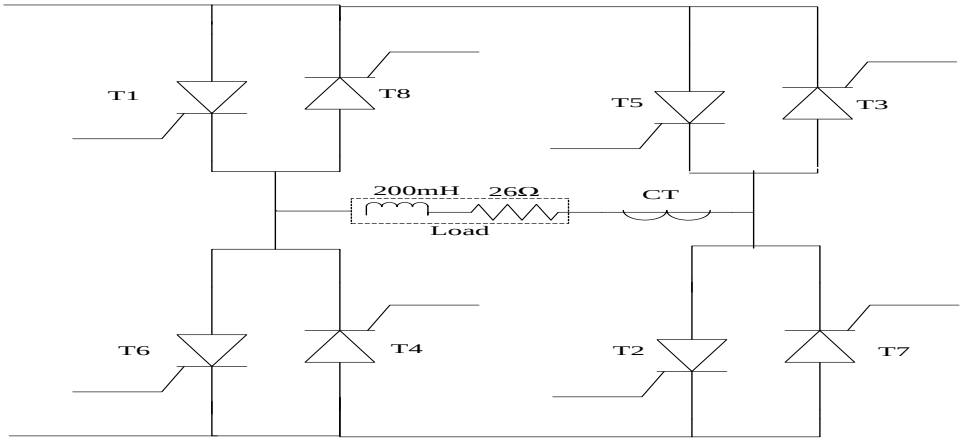

Fig.22 Cycloconverter

Load is inductive load of 200 mH with self resistance of value 26 Ω.

Current transformer is connected to obtain current polarity for feedback. Construction of current transformer is done to achieve ratio of 1:300.

N1I1 = N2I2

2x1A = 600xI2

I2 = 3mA

V = IR

= 3x10-3 x 220 Ω,

= 660mV

Secondary of current transformer is connected with resistance R(220Ω) whose value is chosen such that voltage obtained across R is enough as input to comparator LM311 connected in triggering circuit for selection of positive and negative converter.

vii. ***Design of Thyristor Snubber:***

Let dv/dt = 400 V/μs

L = 25 μH

dv/dt = E*R/L

E = 100V

Where E is secondary voltage peak.

R = 100 Ω

R+R1 = $2\sqrt{L/C}$

Let R1 = 0.02 Ω

C = 0.01 μF

Hence value for snubber chosen is 100 Ω, 1W and 0.01μF/250V.

For heat sink PHS-16 is used as power dissipation is very low.

ISSN 2349-7815

International Journal of Recent Research in Electrical and Electronics Engineering (IJRREEE)
Vol. 2, Issue 1, pp: (32-53), Month: January - March 2015, Available at: www.paperpublications.org

5. SIMULATION & RESULTS

Simulations are done to obtain different gate pulses for different combinations described in table These gate pulses are combined with square wave as HF link voltage to obtain output voltage. (Refer Table 1)

Table 1

Scenario	Carrier Type	Phase Shifter 1	Phase Shifter 2	Phase Shifter 3	Combining Method	Gate Drive Signal Type	Output PWM Equivalent
1	Triangle	0	0	180°	Add	2-Level	Ramp PWM at double fswitch'
2	Triangle	0	180°	0	Subtract	3-Level	Triangle PWM
3	Ramp	0	0	0	Add	2-Level	Triangle PWM
4	Ramp	180°	0	0	Subtract	3-Level	Ramp PWM at double fswitch'

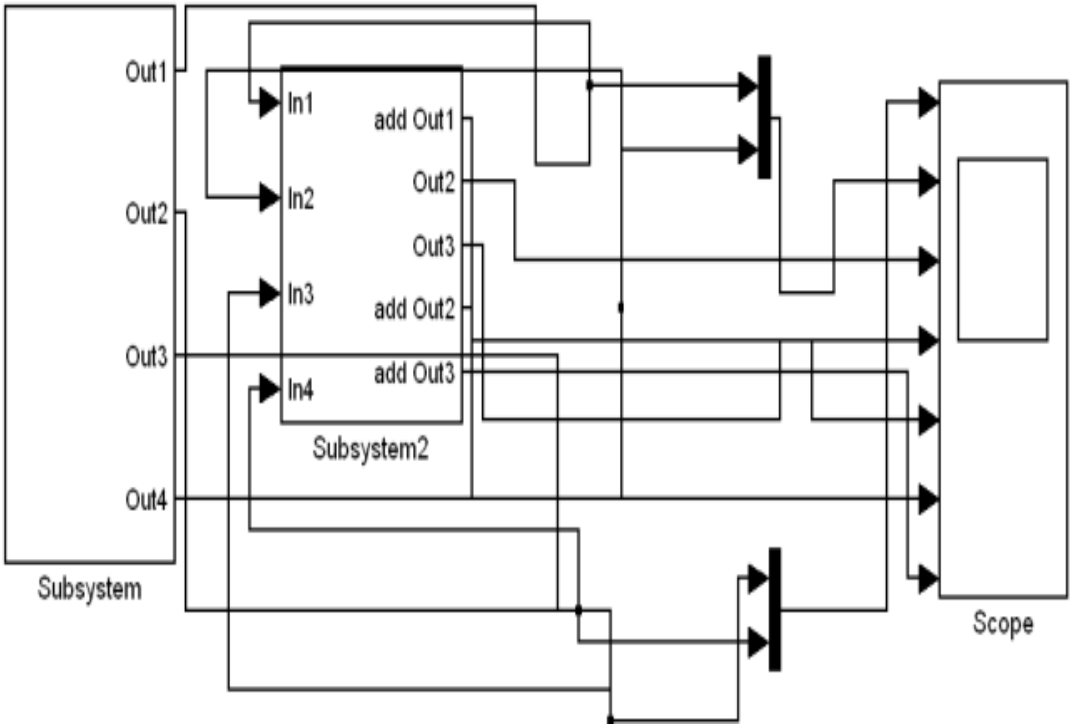

Fig.23 Simulation Block for scenario 1

International Journal of Recent Research in Electrical and Electronics Engineering (IJRREEE)
Vol. 2, Issue 1, pp: (32-53), Month: January - March 2015, Available at: www.paperpublications.org

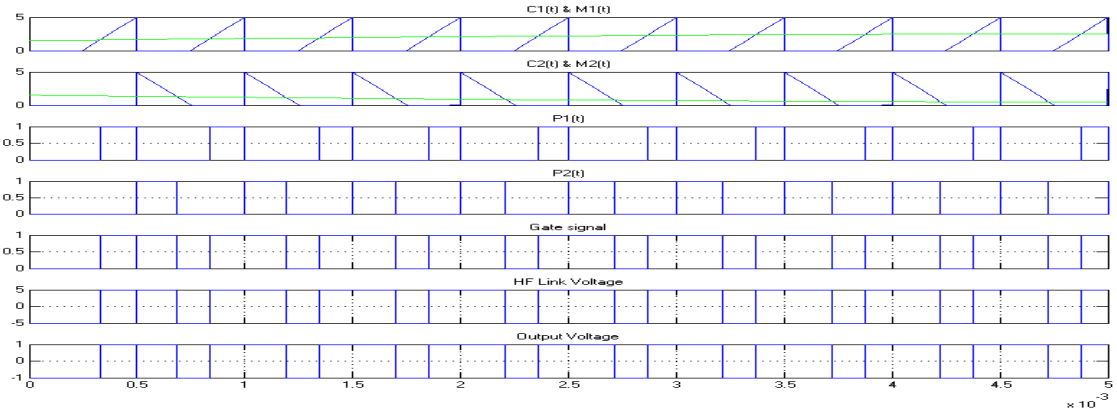

Fig.24 Simulation Result for scenario 1

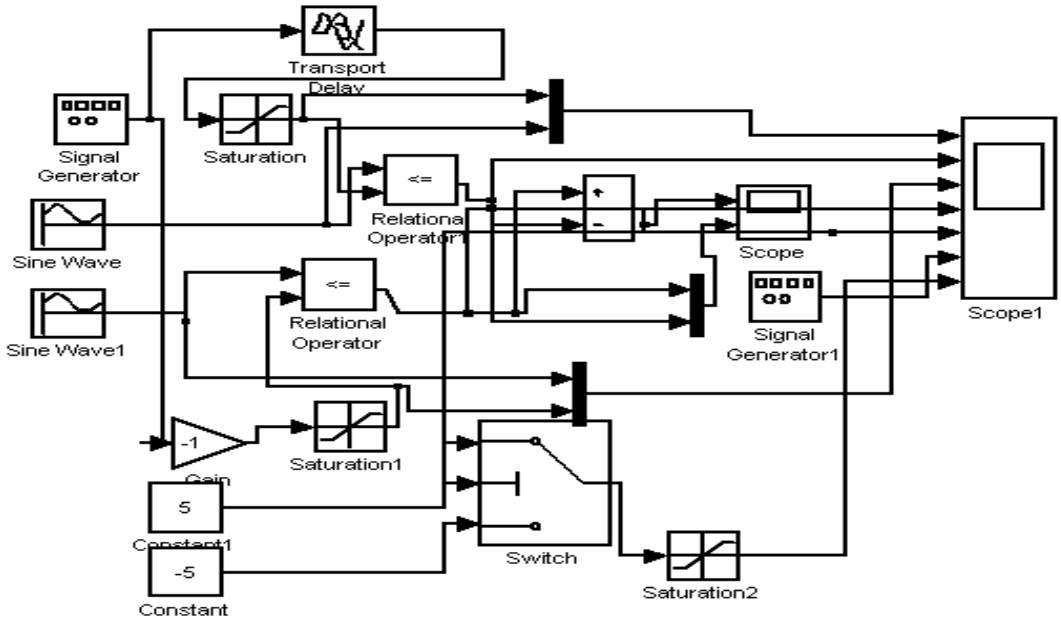

Fig.25 Simulation Block scenario 2

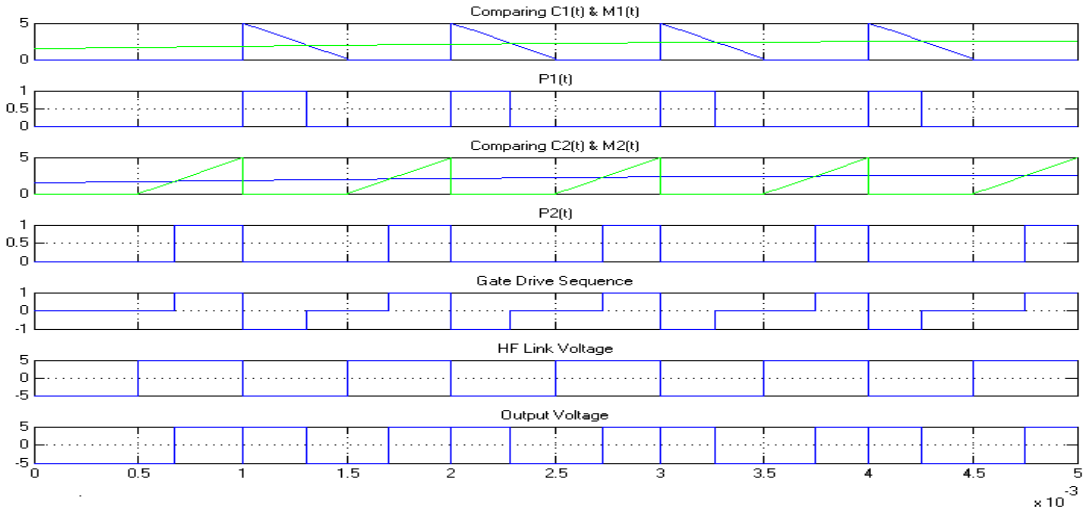

Fig.26 Simulation Result for scenario 2

International Journal of Recent Research in Electrical and Electronics Engineering (IJRREEE)
Vol. 2, Issue 1, pp: (32-53), Month: January - March 2015, Available at: www.paperpublications.org

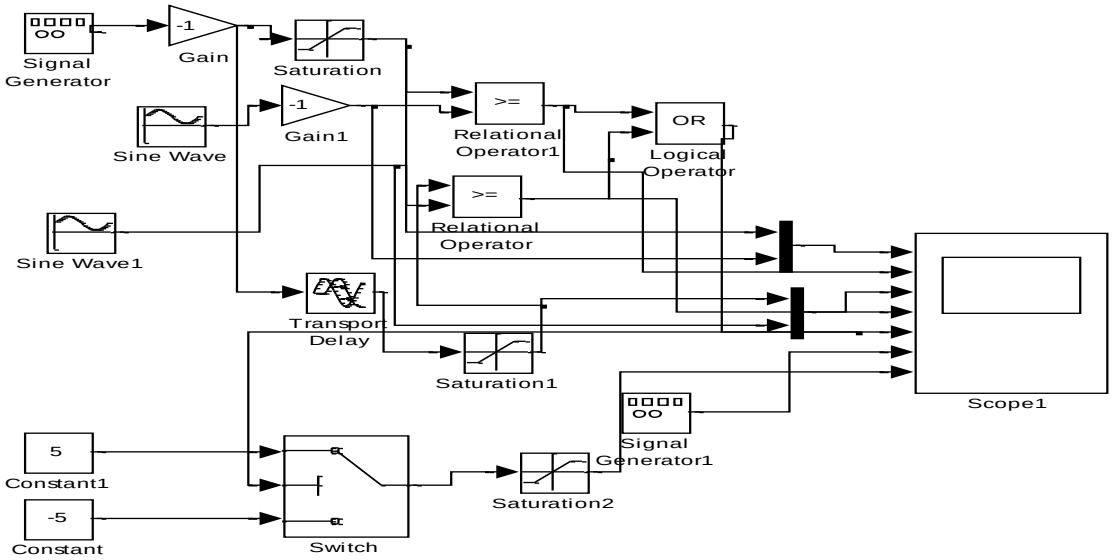

Fig.27 Simulation Block for scenario 3

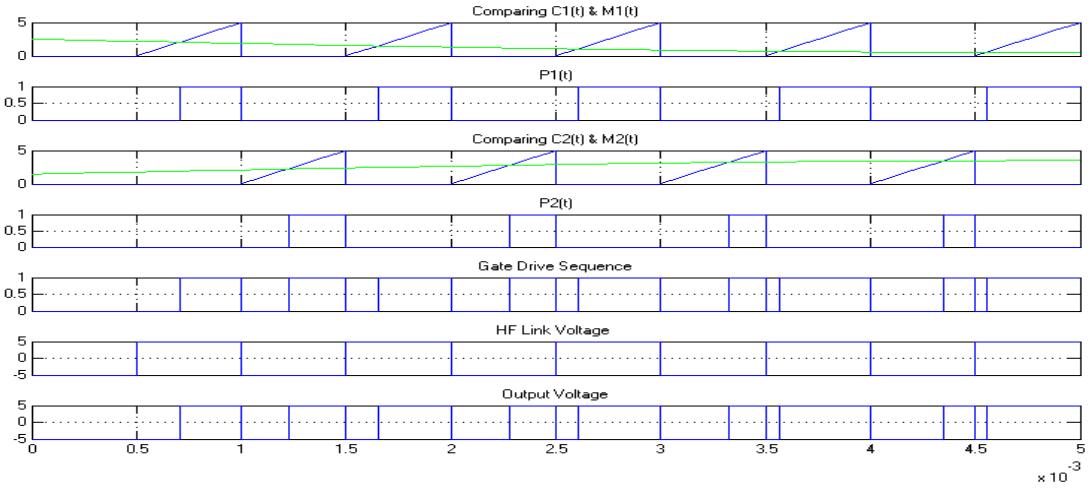

Fig.28 Simulation Result for scenario 3

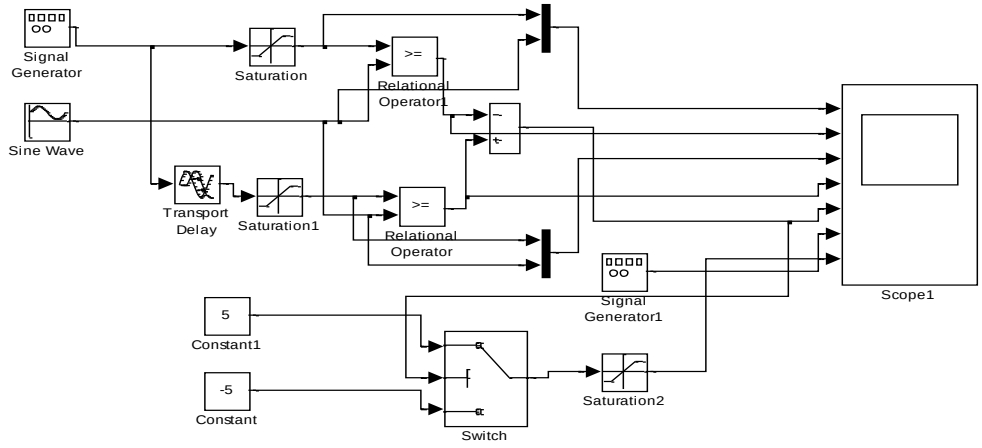

Fig.29 Simulation Block for scenario 4

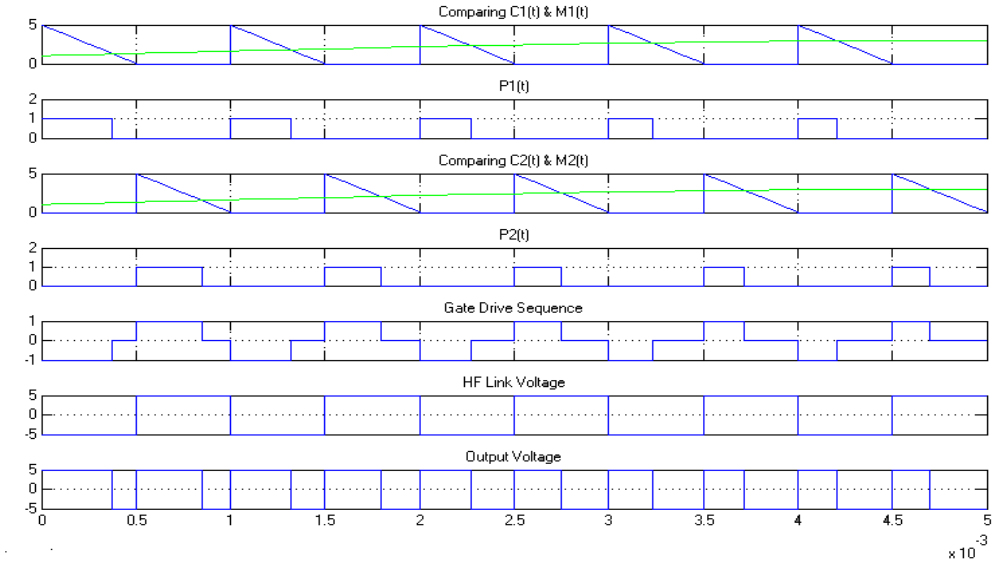

Fig.30 Simulation result for scenario 4

6. CONCLUSION

The scheme suggested shows that the number of stages can be reduced, leading to a HF-link conversion approach. The reduction came from recognizing redundancy in the power processing. Without a dc link bus, rectifiers and filter components along with their associated losses are eliminated. Applying the techniques of multiple carrier PWM cycloconversion results are exactly identical to conventional PWM techniques.

The combination of a current-controlled input, adjust the average power demand from a fuel cell, battery buffer, and PWM cycloconverter, provides a reduced parts-count solution compared to conventional boost-forward-inverter cascade topology. The combined converter isolates the fuel cell from its load both electrically and dynamically while reducing parts count and therefore reduces costs.

REFERENCES

[1] M. Koyama, “High frequency link dc/ac converter with PWM cycloconverter for UPS,” in Proc. IPEC’90 Conf., Tokyo, Japan, 1990, pp. 748–754.

[2] T. Kawabata, K. Honjo, N. Sashida, K. Sanada, and M. Koyama, “High frequency link dc/ac converter with PWM cycloconverter,”in Proc. IEEE Industry Applications Soc. Annu. Meeting, 1990, pp. 1119–1124.

[3] T. Aoki, K. Yotsumoto, S. Muroyama, and Y. Kenmochi, “A new uninterruptible power supply with a bidirectional cycloconverter,” in Proc. IEEE Int. Telecommunications Energy Conf., 1990, pp. 424–429.

[4] J. Kassakian, M. Schlecht, and G. Verghese, Principles of Power Electronics. Reading, MA: Addison-Wesley, 1991, pp. 186–187.

[5] N. H. Kutkut, D. M. Divan, D. W. Novotny, “Charge equalization of series connected battery strings,” IEEE Trans. Industry Applications, vol. 31, no. 3, pp. 562-568, May 1994.

[6] R. D. Brost, “Performance of valve-regulated lead-acid batteries in EV1 extended series strings,” in Proc. 13th Annual Battery Conf. On Applications and Advances, 1998, pp. 25-29.

[7] S. West and P. T. Krein, “Equalization of valve-regulated lead-acid batteries: issues and life test results,” in Proc. IEEE Int. Telecommunications Energy Conf., 2000, pp. 439–446.

[8] S. West, P. T. Krein, "Equalization of valve-regulated lead-acid batteries: issues and life test results," in Proc. IEEE Int'l Telecommunications Energy Conf., 2000, pp. 439-446.

[9] P. T. Krein, "Tricks of the Trade: Simple Solar Cell Models," IEEE Power Electronics Society Newsletter, April 2001.

[10] Fuel cells, IEEE Spectrum. June 2001.

[11] S. Haykin, Communication Systems, 4th ed. New York: Wiley, 2001, p. 211

[12] B. R. Pelly, Thyrister Phase Controlled Converters and Cycloconverters. New York: Wiley-Interscience, 1971.

[13] Op-Amps and Linear Integrated Circuits by Ramamkant A.Gayakwad.